Fachtagung "Experimentelle Strömungsmechanik"
5. – 7. September 2017, Karlsruhe

Cause for a wind-induced damage pattern in the forest edge region

Ursache eines wind-induzierten Schadensmusters im Waldkantenbereich

Christof Gromke*, Bodo Ruck
Laboratory of Building- and Environmental Aerodynamics, Institute for Hydromechanics, Karlsruhe Institute of Technology KIT, Karlsruhe, Germany
*gromke@kit.edu

Key words: forest flow, extreme gust, storm stability, adaptive growth, damage pattern, PIV
Schlagworte: Waldströmung, Extremböe, Sturmstabilität, adaptives Wachstum, Schadensmuster, PIV

Abstract

A particular damage pattern which can occasionally be observed after strong storms shows an intact stripe of trees directly at the windward forest edge and a patch of damaged trees further inside the forest stand (Figure 1). The reason for the occurrence of this damage pattern was unclear in the past and often hypothesized to result from coherent transverse roller structures which develop in the inflection layer in the forest canopy top and adjacent free air region. The present investigation, however, provides evidence that such a damage pattern can be caused by very rare but extremely fast coherent structures, so called extreme gusts, which originate from elevated parts of the atmospheric boundary layer and travel downward to the ground.

Figure 1: Forest damage pattern with an intact stripe of edge trees in a Sitka spruce stand with long-established edge in north-west England. Photo courtesy of Graeme Prest (Forestry Commission, UK).

Introduction

The damage pattern of Figure 1 shows an intact stripe of trees directly at the windward forest edge, and an area of damaged trees further inside of the forest stand. The reason for this damage pattern is still a matter of debate. It is sometimes hypothesized that it results from the breakup of coherent transverse roller structures which develop in the inflection layer in the forest canopy top and adjacent free air region according to the mixing-layer analogy (Finnigan and Brunet 1995; Raupach et al. 1996; Finnigan 2000; Dupont and Brunet 2008, 2009; Finnigan et al. 2009). The present investigation, however, suggests a different reason for the occurrence of this damage pattern. Evidence is provided that it can be caused by a very rare but extremely fast coherent structure, so-called extreme gust. The extreme gust interacts with the flow at the top of the forest canopy to form a vortex (so called primary vortex) which can result in an increased downward momentum transport into the forest canopy at 2 to 4 tree heights h behind the windward edge (Tischmacher und Ruck 2013).

Karlsruhe, Germany, ISBN 978-3-9816764-3-3

Experiment Setup and Measurement Technique

Reduced-scale wind tunnel forest model

Wind tunnel experiments were performed at a reduced-scale forest model (1:200). The forest model had a full-scale height of h = 22 m and extended 7 h in spanwise and 14 h in streamwise direction. It consisted of two distinct horizontal layers, the stem and the crown layer, both 11 m high (Figure 2). The stem layer was realized by ribbed cylindrical wooden dowels arranged in a staggered array. The crown layer was assembled from porous cones made of an open-porous foam material with 10 ppi (pores per inch) which mimicked the characteristic crown shape of needle trees. The aerodynamic similarity was based on the absorption of momentum from the flow. For the stem layer, the criterion involved the drag coefficient and the frontal area index of the tree stems. For the crown layer, the criterion relied on the pressure loss coefficient which describes the normalized continuous pressure decline of flow in a porous medium. The reader is referred to Gromke 2011, Gromke and Ruck 2012, and Gromke and Ruck 2015 for more detailed descriptions of the geometric and aerodynamic similarity criteria.

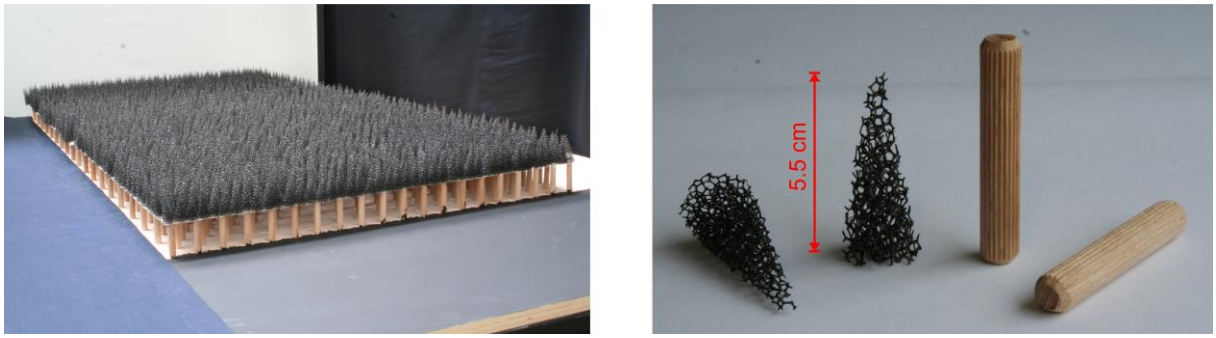

Figure 2: Forest model (left), individual crown and stem layer model elements (right).

Wind tunnel approach flow and extreme gust characteristics

A closed-circuit Goettingen-type wind tunnel with spires and ground-mounted roughness elements installed in the fetch windward of the test section generating a simulated atmospheric boundary layer flow was employed. The measurements were performed with a gradient velocity U_δ = 7.0 m/s and an aerodynamic roughness length z_0 = 0.0014 m. More details on the simulated atmospheric boundary layer flow can be found in Gromke and Ruck 2015. Assuming agricultural land use with mature crops (z_0 = 0.1 … 0.3 m, see e.g. Wieringa 1993, WTG-Merkblatt 1995, Engineering Science Data Unit 2001) windward of the forest as it is typical for Central Europe, the geometric model scale M was determined to M = 1:200.
The extreme gusts were generated by injecting pulsed round jets driven by pressurized air into the simulated atmospheric boundary layer flow (background flow). The injection was controlled by a fast-switching solenoid valve. Full-scale gust durations of 4, 8 and 12 seconds by different pre-pressure levels of compressed air were realized. The simulated extreme gusts entered the background flow through a horizontally aligned straight pipe with an equivalent full-scale diameter of 0.09 h at 5.9 h in front of the windward forest edge at 1.0 h above the ground, where the mean background flow velocity was $U_h = U_{ref}$. Table 1 provides an overview of the simulated extreme gust characteristics. The gust factor $G_{3s,T}$ is defined as the ratio of the maximum 3-second short-time average velocity within the sample interval of duration T to the long-time average velocity of the sample period T. In this study, the long-time average velocity belonging to the interval of duration T was taken as U_{ref}.

exp. no.	valve opening	pre-pressure	U_{ref}	$G_{3s,T}$
-	s	bar	m/s	-
ref.	0	0	3.7	-
1	4	1	3.9	1.45
2	4	2	3.9	1.86
3	8	1	4.0	1.54
4	8	2	3.8	2.26
5	12	1	3.8	1.59
6	12	2	3.7	2.44

Table 1: Characteristics of approaching extreme gusts at x/h = -1.0 and z/h = 1.0.

Particle Image Velocimetry (PIV) system and measurement procedure

A 2D/2C TR PIV system from Dantec Dynamics was deployed for the measurements. The system consisted of a high-speed CMOS sensor with 1280 x 800 pixel resolution and a pulsed dual-cavity, frequency-doubled Nd:YAG laser, see Dantec Dynamics for more details. Recordings were made in the streamwise-oriented spanwise-central vertical plane covering the forest edge region at -2.7 ≤ x/h ≤ 6.2. A PIV recording was synchronously started with the opening of the fast-switching solenoid valve. The double-frame, single-exposure mode was employed with an inter-frame rate of 500 Hz and intra-frame times of 150 ns to ensure a time-resolved acquisition of the transient gust passage. The recordings were evaluated with DynamicStudio from Dantec Dynamics using a 2-step adaptive correlation algorithm (Dantec Dynamics 2013). The final interrogation window size was 32 x 32 pixel by 50% overlap along both dimensions resulting in a full-scale resolution of approximately 1-velocity-vector-per-square-meter. The recording procedure was repeated 50 times and the final evaluations as shown in the next chapter were based on 50 ensemble-averaged velocity field snapshots.

Results and Discussion

Figure 3 shows the normalized extreme instantaneous wind forces $F^{+}_{veg,ext}$ during a gust passage at height z/h = 1.09 above the canopy top for positions 0.0 ≤ x/h ≤ 6.0 for the experiments according to Table 1. For normalization, the extreme instantaneous wind force at the forest edge, i.e. at x/h = 0.0, was taken. Blue plus (+) and red circle (o) symbols represent the normalized maximum positive, i.e. upward-directed, and minimum negative, i.e. downward-directed, extreme wind forces, respectively. The black curve denoted by ‘ref’ shows the normalized extreme wind forces (all positive, i.e. upward-directed) which occurred in the situation of the turbulent boundary layer flow without superimposed gust, i.e. in the reference experiment, see Table 1. The curve is considered to be a measure of the resistance of trees in an established forest stand against failure, either due to windthrow or wind breakage. It represents the trees' resistance in dependence on the distance from the windward forest edge. The approach is in analogy to the principle employed in models for estimating critical wind speeds for tree failure in forest stands (e.g. Gardiner et al. 2000, 2008; Brüchert and Gardiner 2006). The assumption here is that all trees in an established forest stand are at equal risk because of adaptive growth. Trees in an established forest stand are assumed to comply with the position-dependent local wind climate to which they are exposed to because they have adaptively grown. As a result, trees at the forest edge resist higher wind forces

than trees further inside the stand because they are subjected to higher wind speeds. The study by Gardiner et al. (1997) shows a strong decrease in the load within the first two tree heights h behind the forest edge reaching saturation at a distance of approximately three tree heights h. The reference curve employed in this study exhibits similar characteristics. Following an increase close behind the forest edge, it shows a marked decrease in the wind force at up to two to three tree heights and then no significant decrease further downstream.

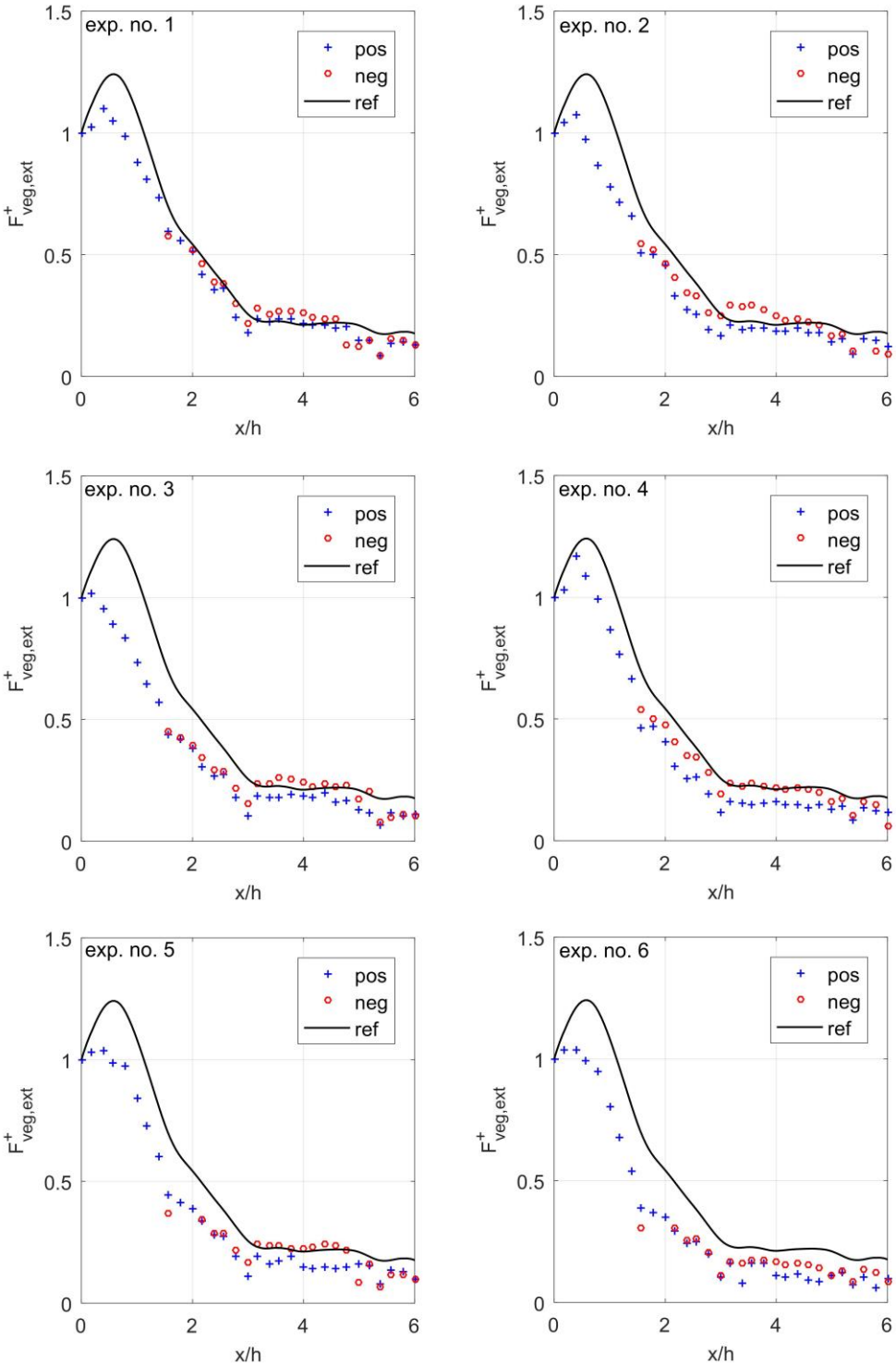

Figure 3: Normalized extreme instantaneous wind forces $F^+_{veg,ext}$ during a gust passage at height z/h = 1.09 for 0.0 ≤ x/h ≤ 6.0.

The normalized extreme wind forces occurring during the gust passages shown in Figure 3 cluster around the reference curve. If they lie below the reference curve, the normalized wind force at canopy top is relatively smaller than it is in the turbulent boundary layer approach flow without superimposed gust. If the normalized extreme wind forces lie above the reference curve, the force is relatively larger than in the case without superimposed gust. On condition that the extreme wind force at the forest edge is just not large enough to cause damage at the first row of trees, the position of the extremes relative to the reference curve implies different damage patterns. Normalized extreme wind forces lying

(i) below the reference curve everywhere imply that no trees have failed,
(ii) above the reference curve everywhere imply that all trees have failed,
(iii) below the reference curve up to a position x_{crit} and above the reference curve for positions $x > x_{crit}$ imply that trees at positions $x \leq x_{crit}$ have not failed but failed for positions $x > x_{crit}$,
(iv) above the reference curve up to a position x_{crit} and below the reference curve for positions $x > x_{crit}$ imply that trees at positions $x \leq x_{crit}$ have failed but not failed for positions $x > x_{crit}$,
(v) below and above the reference curve in alternating sequence imply alternating sections of non-failed and failed trees.

The damage pattern shown in Figure 1 corresponds to the third item. The damage pattern described in the fourth item can be excluded to occur in an established forest stand. It is possible from a pure aerodynamic point of view, however, the failed trees at the established forest edge will leave a new unestablished edge where trees have not adaptively grown to comply with the increased wind forces to which they are suddenly exposed to. In an established forest stand, also the fifth item can be excluded.
The characteristics of the third item are found in experiments no. 1-3 and 5 shown in Figure 3. The normalized extreme forces lie below the reference curve up to a critical position of $x_{crit}/h \approx 3.0$. Normalized extreme wind forces exceeding the reference curve occur only at positions further downstream. With the exception of experiment no. 1, only the normalized negative, i.e. downward-directed, extreme wind forces exceed the reference curve. The extreme wind forces in experiments no. 1-3 and 5 begin to decay at about half a tree height h behind the forest edge. Their decay is relatively less strong compared to that of the trees' resistance as indicated by the reference curve. At approximately $x/h = 3.0$, the normalized extreme forces, in particular the forces acting downward towards the forest canopy, are larger than the trees' resistance. This provides evidence that the damage pattern shown in Figure 1 can originate from the interaction between an extreme gust and the atmospheric boundary layer flow at a forest edge. The interaction leads to the formation of a primary vortex as described by Tischmacher and Ruck (2013). The primary vortex subsequently transports momentum downward into the forest canopy, beginning at approximately 1.5 tree heights h behind the windward edge. The extremes of downward-acting wind forces increase in magnitude in downstream direction and become larger than the trees' resistance at $x/h \approx 3.0$ where they are responsible for tree damage.

Conclusion

The analysis shows that the interaction of an extreme gust with an atmospheric boundary layer flow results in a characteristically different flow and vortex regime in the forest edge region compared to a ‘normal’ atmospheric boundary layer approach flow. The interaction leads to the formation of a vortex (so called primary vortex) at canopy top which intensifies when traveling downstream and subsequently entrains high momentum downward into the forest interior. It is shown that under such conditions the relative decay of downward momen-

Karlsruhe, Germany, ISBN 978-3-9816764-3-3

tum transfer with streamwise direction is less strong than under ‘normal’ atmospheric boundary layer flow conditions. The tree’s resistance with streamwise distance from the forest edge, however, is the result of adaptive growth to wind loads under ‘normal’ flow conditions. At approximately three tree heights h behind the forest edge, the primary vortex induced downward momentum transfer exceeds the adaptively established resistance and leads to tree failure.

Acknowledgements

The financial support of the Deutsche Forschungsgemeinschaft DFG (German Research Foundation) under grant no. Ru 345/30-2 is gratefully acknowledged by the authors.

References

Brüchert, F., Gardiner B., 2006: The effect of wind exposure on the tree aerial architecture and biomechanics of Sitka spruce (Picea sitchensis, Pinaceae). Am J Bot 93:1512–1521
Dantec Dynamics, 2013: DynamicStudio User’s Guide, 660pp
Dupont, S., Brunet, Y., 2008: Edge flow and canopy structure: a large-eddy simulation study. Bound-Layer Meteorol 126:51–71
Dupont, S., Brunet, Y., 2009: Coherent structures in canopy edge flow: a large-eddy simulation study. J Fluid Mech 630:93–128
ESDU, 2001: Characteristics of atmospheric turbulence near the ground, Part II Single point data for strong winds (neutral atmosphere). Eng Sci Data Unit 85020, 42pp
Finnigan, J.J., 2000: Turbulence in plant canopies. Annu Rev Fluid Mech 32:519–571
Finnigan, J.J., Brunet, Y., 1995: Turbulent airflow in forests on flat and hilly terrain. Wind Trees 3–40
Finnigan, J.J., Shaw, R.H., Patton, E.G., 2009: Turbulence structure above a vegetation canopy. J Fluid Mech 637:387–424
Gardiner, B.A., Stacey, G.R., Belcher, R.E., Wood C.J., 1997: Field and wind tunnel assessments of the implications of respacing and thinning for tree stability. Forestry 70:233–252
Gardiner, B., Peltola, H., Kellomäki, S., 2000: Comparison of two models for predicting the critical wind speeds required to damage coniferous trees. Ecol Model 129:1–23
Gardiner, B., Byrne, K., Hale, S., Kamimura, K., Mitchell, S.J., Peltola, H., Ruel, J.C., 2008: A review of mechanistic modelling of wind damage risk to forests. Forestry 81:447–463
Gromke, C., 2011: A vegetation modeling concept for Building and Environmental Aerodynamics wind tunnel tests and its application in pollutant dispersion studies. Environ Pollut 159:2094–2099
Gromke, C., Ruck, B., 2012: Pollutant concentrations in street canyons of different aspect ratio with avenues of trees for various wind directions. Bound-Layer Meteorol 144:41–64
Gromke, C., Ruck, B., 2015: Introduction of a new forest model for wind-tunnel studies and PIV-measurements of flow phenomena at the windward forest edge". Proceedings 23. GALA Fachtagung "Lasermethoden in der Strömungsmesstechnik", Dresden, Germany, p 43.1-8
Raupach, M., Finnigan, J.J., Brunet, Y., 1996: Coherent eddies and turbulence in vegetation canopies: the mixing-layer analogy. Bound-Layer Meteorol 78:351–382
Tischmacher, M., Ruck, B., 2013: Interaction of gusts and forest edges – an experimental wind-tunnel study. Forestry 86:523–532
Wiernga, J., 1993: Representative roughness parameters for homogeneous terrain. Bound-Layer Meteorol 63:323–363
WTG, 1994: WTG-Merkblatt über Windkanalversuche in der Gebäudeaerodynamik. Windtechnologische Gesellschaft, Aachen, 42pp

Karlsruhe, Germany, ISBN 978-3-9816764-3-3